Nonlinear theory of macroscopic flow induced in a drop of ferrofluid

Andrey Yu Zubarev, Dmitry Chirikov, Anton Musikhin, Maxime Raboisson-Michel, Gregory Verger-Dubois, Pavel Kuzhir

Nonlinear theory of macroscopic flow induced in a drop of ferrofluid

Andrey Yu. Zubarev[1,2], Dmitry Chirikov[1], Anton Musikhin[1], Maxime Raboisson-Michel[3,4], Gregory Verger-Dubois[4] and Pavel Kuzhir[3]

[1]Theoretical and Mathematical Physics Department, Institute of Natural Sciences and Mathematics, Ural Federal University, Lenin Ave. 51, Yekaterinburg, 620083, Russia

[2]M.N. Mikheev Institute of Metal Physics, Ural Branch of the Russian Academy of Sciences, Yekaterinburg, 620108, Russia

[3]University Cote d'Azur, CNRS UMR 7010, Institute of Physics of Nice, Parc Valrose, 06108 Nice, France

[4]Axlepios Biomedica, 1 ere Avenue 5e rue, 06510, Carros, France

We present results of theoretical modeling of macroscopic circulating flow induced in a cloud of ferrofluid by oscillating magnetic field. The cloud is placed in a cylindrical channel filled by a nonmagnetic liquid. The aim of this work is development of a scientific basis for a progressive method of address drug delivery to thrombus clots in blood vessels with the help of the magnetically induced circulation flow. Our results show that the oscillating field can induce, inside and near the cloud, specific circulating flows with the velocity amplitude about several millimeters per second. These flows can significantly increase the rate of transport of the molecular non-magnetic impurity in the channel.

1. Introduction

One of the major problems in treatment of brain strokes by injection of the thrombolytic drugs is related to very slow and inefficient transport of the drug to the blood clot because of the absence of the blood flow through the occluded vessel. The US company Pulse Therapeutics has patented the idea of using magnetic nanoparticles allowing significant acceleration of the drug transport [1, 2]. When a dilute suspension of biocompatible magnetic nanoparticles is injected in the blood vessel and alternating magnetic field is applied, the nanoparticles form elongated field-induced aggregates whose periodic translational or angular motion is expected to generate recirculatory flows in the occluded vessel allowing for convective transport of the thrombolytic drug towards the blood clot. Macroscopic experiments on mice suffered from the brain stroke have shown a much better survival rate when nanoparticle treatment was applied [1, 2]. A few recent experimental studies allowing visualization of the clot dissolution in microfluidic channels have recently been published [3, 4], while theoretical analysis of the phenomenon remains scarce [5] so that the fundamental understanding of this problem is still lacking.

For the better understanding of the process of creation of recirculatory flows induced by alternating magnetic fields, we propose in this paper a numerical study of the flows of a magnetic

suspension generated in a long cylindrical channel (mimicking an occluded blood vessel) with the alternating magnetic field created by a pair of coils coaxial with the channel. In the beginning, a drop of the nanoparticle suspension is injected in the center of the channel and a Gaussian concentration profile is assumed at zero time. This study is continuation of our two previous works [6, 7] dealing with a flat channel and covering only short time scales (after setting on the field) when the nanoparticle concentration profile remains unchanged. These first studies demonstrated that efficient recirculatory flows can only be generated in heterogeneous alternating magnetic fields which in their turn induce heterogeneous nanoparticle concentration profiles. The present paper considers the spread of the concentration profile during time and is focused on evolution of the recirculation flows with time. This transient regime shows a decrease of the intensity of the recirculatory flows with time that can affect the efficiency of the brain stroke treatment. From the practical point of view, the characteristic time of this transient has to be compared to the typical time of the medical intervention. We believe that the obtained results will be important for further advancement of this innovative technology.

2. Mathematical model

We consider a cylindrical channel and with two opposite solenoids placed at the extremities along the horizontal axis z, as illustrated in Figure 1.

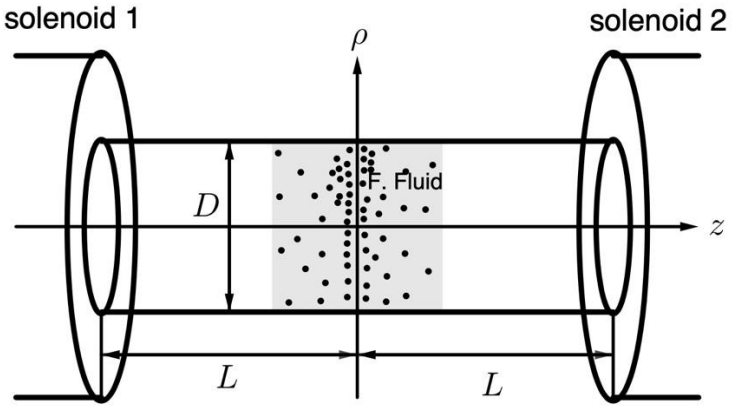

Figure 1. Sketch of a cylindrical channel with a ferrofluid drop (gray rectangle) injected in the middle of the channel. It is supposed that $L<<D$.

The distance $2L$ between the solenoids is supposed to be much larger than the diameter of the cylinder D. The channel is initially filled with a Newtonian liquid. A drop of the ferrofluid with the same liquid carrier as the liquid filling in the channel is introduced in the middle between the solenoids. For

simplicity, we suppose that inside the ferrofluid drop the viscosity η is homogeneous and is the same as outside the drop. This means that at any moment of time, the volume concentration φ of the particles inside the drop is relatively low, about a few volume percent. The initial volume concentration of the particles is supposed to be known and depends only on the coordinate z along the cylinder axis. From the symmetry considerations, we suppose that all physical events are independent of polar angle θ. Then, we consider the linear dependence of the ferrofluid magnetization **M** on the local magnetic field **H**. Note that this approximation is not principal and cannot affect qualitative effects revealed by the present model. The "non-linear" generalization, in principle, is possible, however makes the calculations much more cumbersome.

We suppose that alternating nonuniform magnetic fields $\mathbf{H}_1$ and $\mathbf{H}_2$, created by the solenoids 1 and 2, take the form:

$$\begin{aligned} H_{1z} &= h_{1z}\cos\omega t\,, \qquad H_{1\rho} = h_{1\rho}\cos\omega t, \\ H_{2z} &= h_{2z}\sin\omega t\,, \qquad H_{2\rho} = h_{2\rho}\sin\omega t. \end{aligned} \tag{2.1}$$

where ω is the angular frequency of the alternating magnetic field, t is the time, ρ is the radial coordinate in the cylindrical coordinate system, illustrated in Figure 1.

The components of the field amplitude $\mathbf{h}(z,\ \rho)$, created by the solenoid 1 in Figure 1, are determined the Biot-Savart law [8]:

$$\mathbf{h}_1 = \frac{I_0 N}{4\pi l}\int_{-l-L}^{-L} dz'\left(\int \frac{d\mathbf{s}\times\mathbf{r}'}{|\mathrm{r}'|^3}\right), \tag{2.2}$$

where I_0 is the electrical current amplitude; N is the number of turns of the solenoid; L is the distance between middle of the ferrofluid drop (i.e., origin of the cylindrical coordinate system, shown in Figure 1) and the nearest extremity of the solenoid; l is length of the solenoid; $d\mathbf{s}$ is the differential of the counter of the solenoid wire ring.

In the cylindrical coordinate system, the field $\mathbf{h}_1$ components are:

$$\begin{aligned} h_{1z} &= \frac{I_0 NR}{4\pi l}\int_{-l-L}^{-L} dz'\int_0^{2\pi}\frac{(R-\rho\cos\theta)d\theta}{[(z-z')^2+R^2+\rho^2-2R\rho\cos\theta]^{3/2}}, \\ h_{1\rho} &= \frac{I_0 NR}{4\pi l}\int_{-l-L}^{-L}(z-z')\,dz'\int_0^{2\pi}\frac{\cos\theta\,d\theta}{[(z-z')^2+R^2+\rho^2-2R\rho\cos\theta]^{3/2}}, \end{aligned} \tag{2.3}$$

where R is radius of the solenoid.

Taking into account that the ρ coordinate is small as compared with L, expanding the integrands in (2.3) in the power series with respect to ρ/z, we get the following approximate analytical expressions for the components h_{1z} and $h_{1\rho}$:

$$
\begin{aligned}
h_{1z} &= a_{1z} + \frac{b_{1z}\rho^2}{2}, \qquad h_{1\rho} = a_{1\rho}\rho, \\
a_{1z} &= \frac{I_0 N}{2l}\left[\frac{L+l+z}{\sqrt{(L+l+z)^2+R^2}} - \frac{L+z}{\sqrt{(L+z)^2+R^2}}\right], \\
b_{1z} &= \frac{3I_0 N R^2}{4l}\left\{\frac{L+l+z}{[(L+l+z)^2+R^2]^{5/2}} - \frac{L+z}{[(L+z)^2+R^2]^{5/2}}\right\}, \\
a_{1\rho} &= \frac{I_0 N R^2}{4l}\left\{\frac{1}{[(L+z)^2+R^2]^{3/2}} - \frac{1}{[(L+l+z)^2+R^2]^{3/2}}\right\}.
\end{aligned}
\tag{2.4}
$$

For the second solenoid we get similarly:

$$
\begin{aligned}
h_{2z} &= a_{2z} + \frac{b_{2z}\rho^2}{2}, \qquad h_{2\rho} = a_{2\rho}\rho, \\
a_{2z} &= \frac{I_0 N}{2l}\left[\frac{L+l-z}{\sqrt{(L+l-z)^2+R^2}} - \frac{L-z}{\sqrt{(L-z)^2+R^2}}\right], \\
b_{2z} &= \frac{3I_0 N R^2}{4l}\left\{\frac{L+l-z}{[(L+l-z)^2+R^2]^{5/2}} - \frac{L-z}{[(L-z)^2+R^2]^{5/2}}\right\}, \\
a_{2\rho} &= \frac{I_0 N R^2}{4l}\left\{\frac{1}{[(L+l-z)^2+R^2]^{3/2}} - \frac{1}{[(L-z)^2+R^2]^{3/2}}\right\}.
\end{aligned}
\tag{2.5}
$$

We suppose that the ferrofluid consists of the highly elongated magnetizable particles (mimicking field-induced aggregates composed of spherical ferrofluid nanoparticles). For simplicity we suppose that these elongated particles are always oriented along the local magnetic field **H**. This means that i) the time of the particles reorientation under the alternation field is much less than the field period $2/\omega$ and ii) the angle of the particles deviation from the field under the induced shear flow is very small. Estimates, based on the equations of the particles rotation under the field and flow demonstrate that for realistic situations both of these conditions are fulfilled. The experimental studies on the magnetic colloids designed for the further use in this application show that the field-induced aggregates grow on the timescale of a few seconds up to sizes about 100 μm [9]. For these aggregates the translational or rotational Brownian motion can be safely neglected.

Under these approximations, equations of the fluid flow and continuity of the particles concentration have the forms [10]:

$$-\nabla p + \eta\Delta\mathbf{u} + \varphi\mathbf{F}_m = 0, \qquad \mathrm{div}\mathbf{u} = 0, \qquad \frac{\partial\varphi}{\partial t} + \mathrm{div}\mathbf{j} = 0, \qquad \mathbf{j} = \varphi\boldsymbol{\beta}\cdot\mathbf{F}_m v_p + \varphi\mathbf{u}. \tag{2.6}$$

Here, **u** is the suspension flow velocity; p is the pressure; φ is volume concentration of the particles; **j** is the flux density of the concentration φ; $\mathbf{F}_m$ is the magnetic force per unit volume of the particle by the magnetic field gradient; v_p is the particle volume; $\boldsymbol{\beta}$ is the hydrodynamic mobility tensor of the elongated particle along the force $\mathbf{F}_m$. Note that the inertia term with $d\mathbf{u}/dt$ is not included in the first equation of (2.6), since, as estimates show, in the realistic situations this term is small as compared with the other terms of this equation.

In the frames of the linear magnetization approximation, the magnetic force acting by a unit volume of the elongated particle, can be estimated as follows [11]:

$$\mathbf{F}_m = -\nabla U, \qquad U = -\frac{\mu_0\chi_p H^2}{2\left(1+\chi_p n\right)}. \tag{2.7}$$

Here U is the potential energy of elongated particles oriented at each point along the local the field $\mathbf{H}(z, \rho, t)$ and evaluated under realistic approximation of high length-to-diameter ratio of particles; χ_p is magnetic susceptibility of these particle; $\mu_0 = 4\pi \times 10^{-7}$ H/m is magnetic permeability of vacuum; n is the particle demagnetizing factor. For elongated particles, the following formula can be used:

$$n = \frac{1}{r^2-1}\left[\frac{r\ln\left(r+\sqrt{r^2-1}\right)}{\sqrt{r^2-1}} - 1\right] \approx \frac{\ln(2r)-1}{r^2}. \tag{2.8}$$

Here r is the particle aspect ratio (ratio of the major to the minor axis) of the particle. For $r = 10$ the strong inequality $n << 1$ is held.

Analyses shows that sign of the radial component $F_{m\rho}$ of the magtnetophoretic force $\mathbf{F}_m$ oscillates with time. However the average, over time, component acts towards the channel axis (see below eq. (2.14)). Thus it provokes appearance of the cylindrical zone of the densely packed particles around the axis (see Figure 2). Equation of the layer thickness h growth reads:

$$j_\rho = (\varphi_* - \varphi)\frac{dh}{dt}, \text{ at } \rho = 0. \tag{2.9}$$

Here φ_* is the dense packing volume concentration. For the long cylindrical rods it can be estimated as $\varphi_* \approx 0.785$ and $\varphi_* \approx 0.907$ at the ideal dense quadratic and ideal and hexagonal packing respectively. Of course, with respect to the real suspensions, these estimates can be considered only as the first approximation.

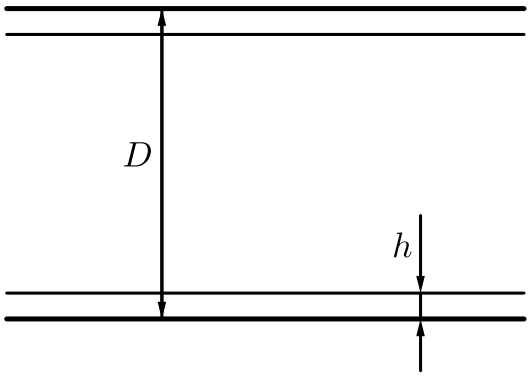

Figure 2. Sketch of the layer thickness *h*.

Applying the ***rot*** operator to both parts of the first equation in (2.6), one gets:

$$\mathrm{rot}\Delta\mathbf{u} = \frac{1}{\eta}\mathrm{rot}(\varphi\nabla U). \tag{2.10}$$

Let us introduce the standard stream function ψ:

$$u_z = \frac{1}{\rho}\frac{\partial(\rho\psi)}{\partial\rho}, \qquad u_\rho = -\frac{\partial\psi}{\partial z}. \tag{2.11}$$

which satisfies the incompressibility equation div**u** = 0. By using (2.10), (2.11) in (2.7), we come to the following relation:

$$\frac{\partial^4\psi}{\partial z^4} + 2\frac{\partial^2}{\partial z^2}\left(\frac{\partial^2\psi}{\partial\rho^2} + \frac{1}{\rho}\frac{\partial\psi}{\partial\rho} - \frac{\psi}{\rho^2}\right) + \frac{\partial}{\partial\rho}\left\{\frac{1}{\rho}\frac{\partial}{\partial\rho}\left\{\rho\frac{\partial}{\partial\rho}\left[\frac{1}{\rho}\frac{\partial(\rho\psi)}{\partial\rho}\right]\right\}\right\} = \\ = \frac{1}{\eta}\left(\frac{\partial\varphi}{\partial\rho}\frac{\partial U}{\partial z} - \frac{\partial\varphi}{\partial z}\frac{\partial U}{\partial\rho}\right). \tag{2.12}$$

Since the inequality $D << L$ is held, all derivatives of ψ over ρ are much larger than the derivatives over z.

Taking it into account, the equation (2.12) is reduced as:

$$\frac{\partial}{\partial\rho}\left\{\frac{1}{\rho}\frac{\partial}{\partial\rho}\left\{\rho\frac{\partial}{\partial\rho}\left[\frac{1}{\rho}\frac{\partial(\rho\psi)}{\partial\rho}\right]\right\}\right\} = \frac{1}{\eta}\left(\frac{\partial\varphi}{\partial\rho}\frac{\partial U}{\partial z} - \frac{\partial\varphi}{\partial z}\frac{\partial U}{\partial\rho}\right), \text{ at } h<\rho<. \tag{2.13}$$

By using the relations (2.1), (2.4) (2.5) and (2.7), keeping only the linear term with respect to ρ/L coordinate, one gets:

$$\frac{\partial U}{\partial \rho} = -a_U \rho,$$

$$a_U = \mu_0 \chi_a \left[\left(a_{1z} b_{1z} + a_{1\rho}^2\right) \cos^2 \omega t + \left(\frac{a_{1z} b_{2z} + a_{2z} b_{1z}}{2} + a_{1\rho} a_{2\rho} \right) \sin(2\omega t) + \right.$$
$$\left. + \left(a_{2z} b_{2z} + a_{2\rho}^2\right) \sin^2 \omega t \right],$$

$$\frac{\partial U}{\partial z} = -\frac{\mu_0 \chi_p (a_{1z} \cos \omega t + a_{2z} \sin \omega t)}{1 + \chi_p n} \left(\frac{\partial a_{1z}}{\partial z} \cos \omega t + \frac{\partial a_{2z}}{\partial z} \sin \omega t \right), \tag{2.14}$$

$$\frac{\partial a_{1z}}{\partial z} = \frac{I_0 R^2}{2l} \left\{ \frac{1}{[(L + l + z)^2 + R^2]^{3/2}} - \frac{1}{[(L + z)^2 + R^2]^{3/2}} \right\},$$

$$\frac{\partial a_{2z}}{\partial z} = \frac{I_0 R^2}{2l} \left\{ \frac{1}{[(L - z)^2 + R^2]^{3/2}} - \frac{1}{[(L + l - z)^2 + R^2]^{3/2}} \right\}.$$

Estimates, based on (2.6) a and (2.9) indicate that for all times interval, presenting interest, the thickness h of the central bulk zone remains negligible as compared with the channel radius *D/2*. Therefore, it can be safely put equal to zero in all simulations. In this approximation the boundary conditions for the function ψ are:

$$\frac{\partial \psi}{\partial z} = 0, \qquad \frac{1}{\rho} \frac{\partial (\rho \psi)}{\partial \rho} = 0, \text{ at } \rho = \frac{D}{2} - h.$$

$$|\psi| < \infty, \qquad \left| \frac{1}{\rho} \frac{\partial (\rho \psi)}{\partial \rho} \right| < \infty, \qquad \left| \frac{\partial}{\partial \rho} \frac{1}{\rho} \frac{\partial (\rho \psi)}{\partial \rho} \right| < \infty, \text{ at } \rho = 0, \tag{2.15}$$

$$\psi \to 0, \qquad z \to \pm\infty.$$

Taking into account that at the infinitely long distance from the ferrofluid drop the fluid must be motionless, i.e., the condition $u \to 0$ at $z \to \pm\infty$ is fulfilled, we can put $\psi \equiv const$ at the infinity from the drop. The concrete magnitude of this *const* does not have a physical meaning. Thus, we put *const* = 0. The first boundary condition in (2.15) shows that on the channel boundary (at $\rho = D/2 - h$) the stream function ψ does not depend on z. Therefore, for this problem the condition $\partial\psi/\partial z = 0$ is identical with the $\psi = 0$ at $\rho = D/2$. The last is simpler for the calculations. Note, that because the fluid incompressibility, the condition $\psi \to 0$ at $z \to \pm\infty$ is identical with the condition of zero flow rate across the channel at any coordinate z.

The components of the mobility tensor $\boldsymbol{\beta}$ in eq. (2.6) can be presented as (see, for example, [12]):

$$\beta_{\parallel} = \frac{\gamma(r) + r^2\alpha_1(r)}{8\pi\eta d_p}, \qquad \beta_{\perp} = \frac{\gamma(r) + \alpha_2(r)}{8\pi\eta d_p},$$
$$\gamma(r) = \int_0^{\infty} \frac{dx}{(1+x)\sqrt{r^2+x}} \approx \frac{2\ln(2r)}{r},$$
$$\alpha_1(r) = \int_0^{\infty} \frac{dx}{(1+x)(r^2+x)^{3/2}} \approx \frac{2[\ln(2r)-1]}{r^3}, \tag{2.16}$$
$$\alpha_2(r) = \int_0^{\infty} \frac{dx}{(1+x)^2\sqrt{r^2+x}} \approx \frac{1}{r}.$$

Here r is the particle aspect ratio (ratio of the major to the minor axis) of the particle, $\beta_{\parallel}$ and $\beta_{\perp}$ are the mobilities in the directions along and perpendicular to the particle axes, d_p is the particle diameter (minor axis). For $r = 1$ (spherical particle) $\beta_{\parallel} = \beta_{\perp} = 1/(3\pi\eta d_p)$, as it should be according to the classical Stokes formula. In the range of the aspect ratio $10 < r < 100$, presented interest from the point of view of the application the values of $\beta_{\parallel}$ and $\beta_{\perp}$ differ non significantly (see Figure 3).

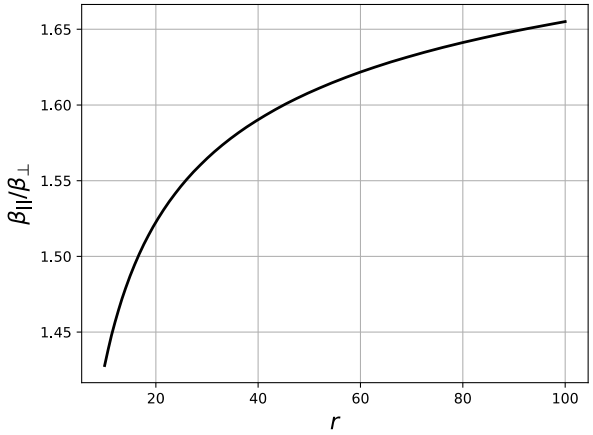

Figure 3. The ratio $\beta_{\parallel}/\beta_{\perp}$ vs. the aspect parameter r.

That is why below we will use the scalar value $\beta(r) = [\beta_{\parallel}(r) + \beta_{\perp}(r)] / 2$.

The partial differential nonlinear equation for the concentration φ taking into account the continuity equation has the form:

$$\frac{\partial\varphi}{\partial t} + u_{\rho}\frac{\partial\varphi}{\partial\rho} + u_z\frac{\partial\varphi}{\partial z} - \frac{\beta v_p}{\rho}\frac{\partial}{\partial\rho}\left(\rho\varphi\frac{\partial U}{\partial\rho}\right) - \beta v_p\frac{\partial}{\partial z}\left(\varphi\frac{\partial U}{\partial z}\right) = 0, \text{ at } \rho < \frac{D}{2}. \tag{2.17}$$

Solution of this equation depends on the initial conditions. To be specific, we choose here the condition in the form:

$$\varphi = \varphi_0 e^{-\frac{z^2}{\sigma^2}}, \qquad t = 0, \tag{2.18}$$

where σ the typical length of the ferroparticles cloud. Note that the initial condition like (2.18) corresponds namely to some cloud of the particles, injected into the channel being suspended in some soluble liquid, not to a drop ofan insoluble ferrofluid, which can form a new thrombus in the blood channel.

Differential equation (2.6), (2.13) and (2.17) can be solved numerically using an implicit difference scheme.

3. Results

Figure 4 demonstrates evolution of the concentration profile with time. It is clearly seen that concentration profile of the ferrofluids is blurred. Physically it takes place because of the magnetophoretic and convective motion of the particles. Our estimates show that, for the studied system, the convective motion dominates over the magnetophoretic one.

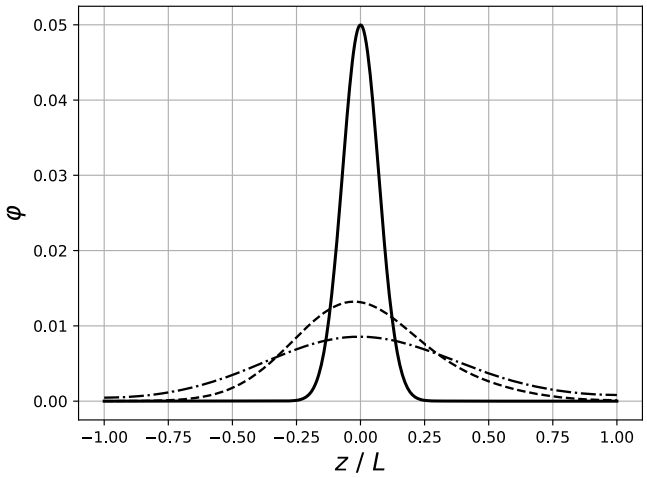

Figure 4. The distribution of concentration φ along the axis coordinate z. The solenoid parameters are: radius R = 10cm; length l = 5cm; the product I_0N = 18kA; the current angular frequency ω = 15 rad/s; the distance between the solenoids $2L$ = 20cm; the diameter of the cylinder D = 5mm; magnetic susceptibility of elongated particles χ_a = 25; the viscosity of water η = 1mPa·s; φ_0 = 0.05; the typical length of a cloud of ferroparticles σ = 1cm; the amplitude of the magnetic field H = 32 kA/m. Black solid line – distribution of concentration at t = 0; dash line – distribution of concentration at time t = 20 sec; dash-dotted line – distribution of concentration at time t = 1 min.

Some results of calculations of the longitudinal component of the velocity u_z at the axis of the cylinder (ρ = 0) are shown in Figure 5. The results demonstrate that, for the chosen parameters of the

system, at the onset of the process, the longitudinal velocity u_z, can achieve several millimeters per second near points of maximum of the particles concentration gradient; with time u_z decreases. This velocity decrease is explained by the concentration profile blurring.

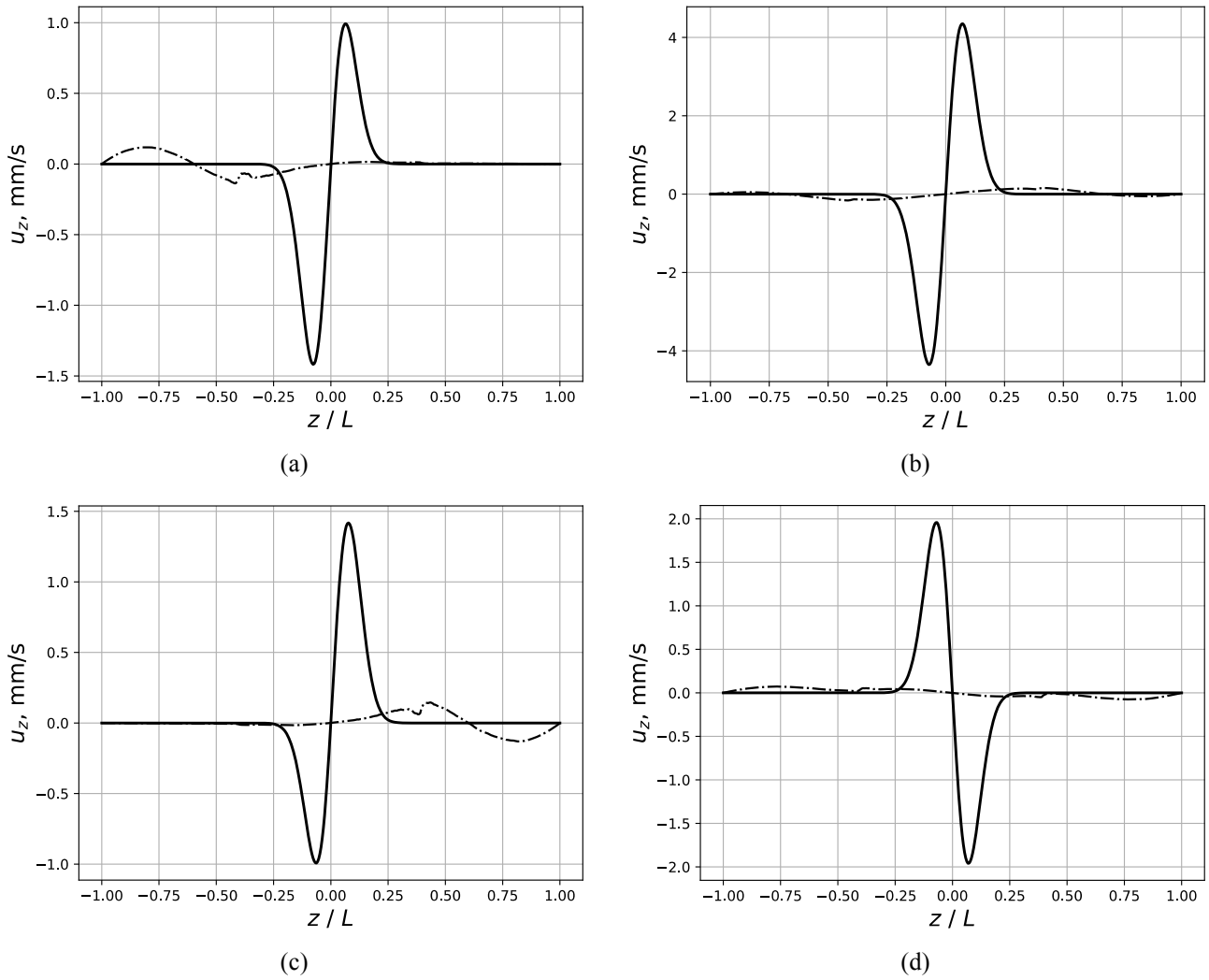

Figure 5. The longitudinal velocity u_z at the axis of the cylinder vs. coordinate z for several moments of time: (a) $t = t_0$; (b) $t = t_0 + T/8$; (c) $t = t_0 + T/4$; (d) $t = t_0 + 3T/8$; $T = 2\pi/\omega$. The other parameters of the system are the same as in Figure 4. Black solid line $t_0 = 0$; dash-dotted line – $t_0 = 1$ min.

The illustration of the vector velocity field (see Figure 6) shows that the strong inequality $u_\rho << u_z$ holds very well.

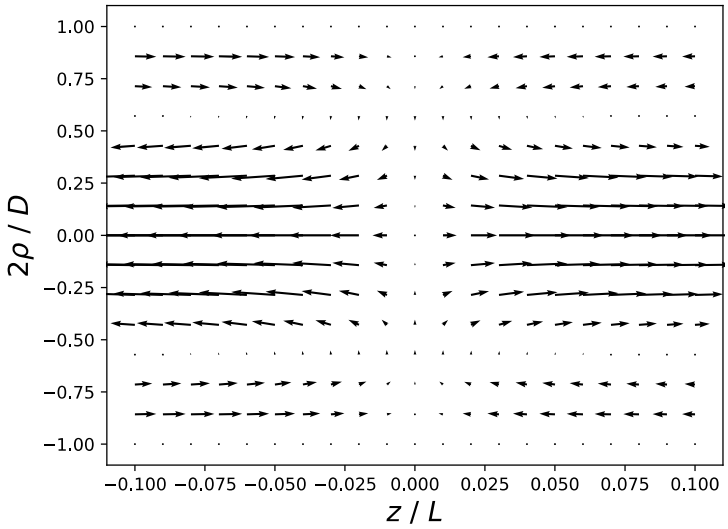

Figure 6. The illustration of the direction and rate of the fluid velocity in the channel.

4. Conclusion

In the present paper, we simulated recirculating flows inside a heterogeneous suspension of elongated magnetic particles (or field-induced nanoparticle aggregates) inside a cylindrical channel placed in a nonuniform alternating magnetic field. The model is based on equation of fluid motion coupled with an equation for the convective transport of particles. The generation of recirculating flow is possible thanks to the magnetic particle migration induced by the field gradient while the periodic change of the velocity direction is ensured by the variation of the field with time. Our results show that the running oscillating field with a quite realistic amplitude can induce circulating flows with the velocity amplitude about several millimeters per second during initial moments after the field application. However, on the timescale of about one minute, the suspension flow velocity becomes much less than at the initial time ρ. The reason for this decrease is the spreading of the concentration profile. We believe this work to be useful for the understanding of the process of blood clot dissolution assisted by continuous drug delivery with the help of field-induced recirculating flows. Note, that at this stage we consider the model situation, which can be experimentally checked and studied the *in-vitro* conditions. The study of the situation close to *in-vivo* situation will be the next stage of our work in this field

Funding. AZ and DCh thanks the Russian Science Foundation, project 20-12-00031, for the financial support. PK and MRM thank the funding of French ‘Agence Nationale de la Recherche’, Project Future

Investments UCA JEDI, No. ANR-15-IDEX-01 (projects ImmunoMag and MagFilter) and by the private company Axlepios Biomedicals.

References

1. Creighton FM. 2012 Magnetic-based systems for treating occluded vessels. U.S. Patent No. 8,308,628.

2. Creighton FM, Sabo M, Null C, Epplin G, Wachtman JC (2018). U.S. Patent No. 9,883,878.

3. Gabayno JLF, Liu DW, Chang M, Lin YH. 2015 Controlled manipulation of Fe3O4 nanoparticles in an oscillating magnetic field for fast ablation of microchannel occlusion. *Nanoscale* **7**, 3947-3953. (doi:10.1039/C4NR06143H)

4. Li Q, Liu X, Chang M, Lu Z. 2018 Thrombolysis enhancing by magnetic manipulation of Fe3O4 nanoparticles. *Materials* **11**, 2313. (doi:10.3390/ma11112313)

5. Clements MJ. 2016 A mathematical model for magnetically assisted delivery of thrombolytics in occluded blood vessels for ischemic stroke treatment. Doctoral dissertation, Texas University.

6. Musickhin A, Zubarev A, Raboisson-Michel M, Verger-Dubois G, Pavel Kuzhir P. 2020 Field-induced circulation flow in magnetic fluids. *Phil. Trans.* R. Soc. A **378**: 20190250. (doi:10.1098/rsta.2019.0250)

7. Zubarev A, Raboisson-Michel M, Verger-Dubois G, Kuzhir P. 2020 To the theory of ferrohydrodynamic circulating flow induced by running magnetic field. *Eur. Phys. J.* Special Topics **229**, 2961–2966. (doi:10.1140/epjst/e2020-000119-3)

8. Purcell EM., 1985 Electricity and Magnetism (Berkeley Physics Course, Vol. 2) McGraw Hill.

9. Raboisson-Michel M, Queiros Campos J, Schaub S, Zubarev A, Verger-Dubois G, Kuzhir P. 2020 Kinetics of field-induced phase separation of a magnetic colloid under rotating magnetic fields. *The Journal of Chemical Physics* **153**(15), 154902 (doi:10.1063/5.0023706)

10. Rosensweig R. 1985 Ferrohydrodynamics. Cambridge, New York: Cambridge University Press.

11. Landau L, Lifshitz E. 1960 Electrodynamics of continuum media. London, UK: Pergamon Press.

12. Theo van de Ven G. 1989 Colloidal Hydrodynamics. London, UK: Academic Press.